Paper No.
MCI14

Ethyl 6-amino-4-(methoxyphenyl) 3methyl2,4-dihydropyrano [2,3,C] pyrazole-5-carboxylate as novel corrosion inhibitors for mild steel in Hydrochloric Acid Solution useful for industrial pickling process

Parul Dohare

Department of Chemistry, Indian Institute of Technology,
paruldohare.17@gmail.com

M. A. Quraishi

Banaras Hindu University, Varanasi 221 005 (INDIA)
dparul.rs.apc13@itbhu.ac.

ABSTRACT

In the present work a new corrosion inhibitor namely Ethyl 6-amino-3-methyl-4-(methoxyphenyl) 2,4-dihydropyrano [2,3,C] pyrazole-5-carboxylate (MEP), was prepared, characterized and corrosion inhibition properties was investigated on mild steel using gravimetric, potentiodynamic polarization, electrochemical impedance spectroscopy (EIS), Scanning electron microscopy (SEM), Atomic force microscopy (AFM) and theoretical methods. MEP exhibited highest efficiency of 98.8 % at 100 mg/L. AFM and SEM studies confirmed formation of adsorbed film on the metal surface and followed Langmuir adsorption isotherm. The DFT and MD which further corroborated the experimental results.

Keywords: Mild steel, EIS, SEM, AFM

INTRODUCTION

In oil and gas production industries, mild steel is widely used [1]. Hydrochloric acid is often used in industries for the removal of rust, acid cleaning, de-scaling, etc. One of the major problems of using hydrochloric acid is the damage caused by corrosion. In order to prevent damage, organic inhibitors having heteroatoms like N, O and S are commonly used [2-4].The adsorption of these organic molecules on metals surfaces depends mainly on the nature and the surface charge of metals, the chemical structure of organic molecule (functional groups, steric factors, electron density, etc) and the type of solution [5-7].The adsorption mechanism of the inhibitor over the metal solution interface takes place through the replacement of water molecules according to the following equation:
$Inh_{(sol)} + xH_2O_{(ads)}$ $Inh_{(ads)} + xH_2O_{(sol)}$

In this equation, $Inh_{(sol)}$ and $Inh_{(ads)}$,both are inhibitor molecules in the solution, and are adsorbed on the metal surface. 'x' is the number of water molecules replaced by inhibitor molecule.

Pyranpyrazole are important class of compounds that includes pharmaceuticals and exhibit various biological activities like anticancer, anti bacterial and anti inflammatory activities. Because of their wide range of pharmaceuticals applications they are produced in large quantity [8]. Survey of literature showed there are a few reports on use of pyranopyrazole derivatives as corrosion inhibitors for mild steel in hydrochloric acid Yadav et al [9] reported 5- carbonitrile substituted dihydropyranopyrazole derivatives. The compounds exhibited 88 to 98% inhibition efficiency at 300 mg/L. DFT and MD have been used to study the chemical reactivity and adsorption behavior of the inhibiting molecules on metal surface [10]. In the present work we have studied the corrosion inhibition performance and adsorption behavior of Ethyl 6-amino-4-(methoxyphenyl) 3methyl2,4-dihydropyrano [2,3,C] pyrazole-5-carboxylate as corrosion inhibitor for mild steel in 1M HCl solution. The corrosion inhibition tests were performed on mild steel in acidic medium using potentiodynamic polarization, electrochemical impedance spectroscopy, and gravimetric, surface SEM by scanning electron microscopy (SEM) and atomic force microscopy (AFM). The theoretical calculation using density functional theory (DFT) and the molecular dynamics simulation were also used to establish correlation between molecular structures and IE.

1. EXPERIMENTAL PROCEDURE

2.1. Materials

2.1.1. Material and test solution

The tested inhibitor was synthesized as reported in the literature [11]. For all Gravimetric measurement, electrochemical experiments, and surface studies the mild steel specimens were cut from the commercially available mild steel sheet having chemical composition (weight percentage): C (0.076), Mn (0.192), P (0.012), Si (0.026), Cr (0.050), Al (0.023), and Fe (balance). The exposed surface of the working electrodes was cleaned successively with emery papers of different grade (600, 800, 1000, 1200), washed with deionized water, degreased with acetone, ultrasonically cleaned with ethanol and stored in moisture free desiccators before used in the experiments. Test solution was 1M HCl for weight loss, electrochemical and surface measurement which was prepared by dilution of an analytical reagent grade 37% HCl in double deionized water.

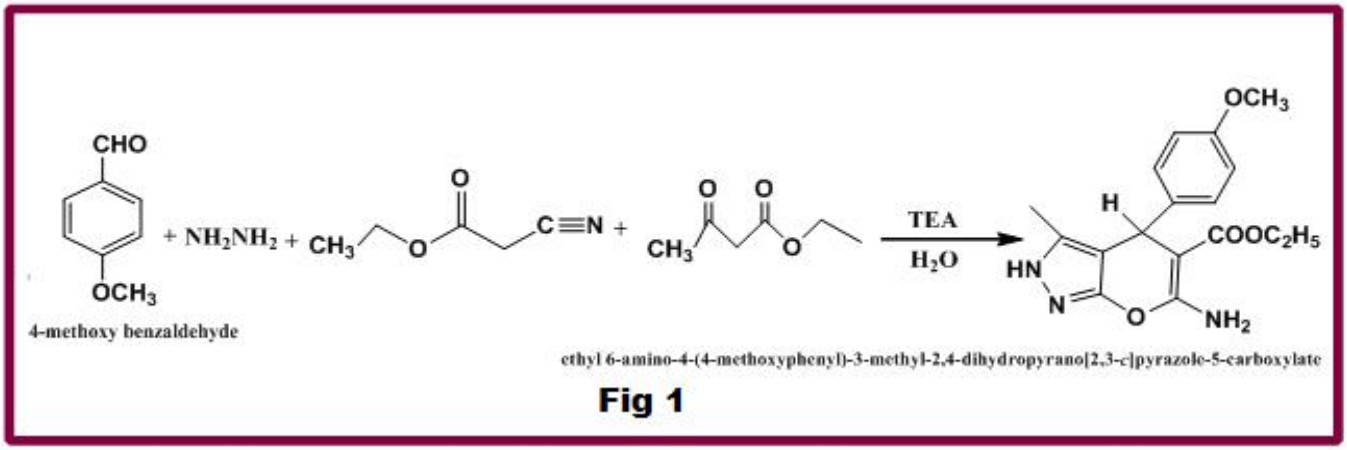

Fig 1

Table 1: Molecular structure and abbreviation

Inhibitor	Structure
(Ethyl 6-amino-4-4(methoxyphenyl-3-methyl2,4dihydropyrano[2,3,C]pyrazole-5-carboxylate (MEP)	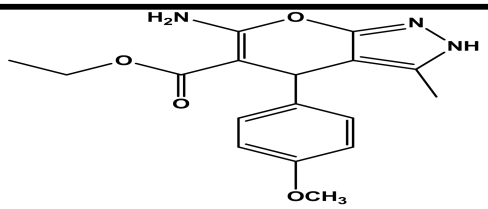

2.1.2. Gravimetric measurement

Gravimetric experiment was performed according to ASTM standard method [12]. The corrosion rates CR (mg cm2 h-1) were calculated using equations.

$$C_{\mathrm{R}} = \frac{W}{At} \tag{1}$$

Here, *W* is the weight loss of mild steel coupon, *A* is the total area of mild steel coupon and *t* is immersion time (3h). With the calculated corrosion rate, the inhibition efficiency *η* % was calculated as follows:

$$\eta\% = \frac{C_R - C_{R(i)}}{C_R} \times 100 \tag{2}$$

Surface coverage (*θ*) values were calculated by the following equation:

$$\theta = \frac{C_{\mathrm{R}} - C_{\mathrm{R(i)}}}{C_{\mathrm{R}}} \tag{3}$$

2.1.3. Electrochemical measurement

The electrochemical study was conducted in the three-electrode cell assembly, using mild steel strip as working electrode (with an exposed area of 1cm^2), graphite rod as counter electrode and saturated calomel electrode (SCE) as reference electrode. The electrochemical measurements were carried out using a Gamry Potentiostat/Galvanostat (Model G-300) connected to a personal computer with EIS software Gamry Instruments Inc., USA. The electrochemical experiments were analyzed by electrochemical software Echem Analyst 5.5 Software package. The EIS measurement was carried in the frequency range of 10^6 Hz to 10^{-2} Hz at open circuit potential (OCP). All the experiments were performed after immersion of MS for 30 min in 1 M HCl in absence and presence of inhibitors. Potentiodynamic polarization curves were obtained by shifting the electrode potential automatically from - 250 mV to + 250 mV vs. OCP at a scan rate of 1 mV/s. All electrochemical experiments were performed at 308 K temperature.

2.1.4. Surface analysis

The surface study of mild steel coupons was analyzed using scanning electron microscope (SEM) and atomic force microscope (AFM) by immersing the metal in 1.0 M HCl in absence and presence of inhibitors for 24 h at 308 K. SEM images were performed at the at magnification of 5Kx and accelerating voltage of 5KV using a Ziess Evo 50 XVP instrument. AFM analysis was done using NT-MDT multimode, Russia, controlled by solver scanning probe microscope controller.

2.1.5. Quantum chemical calculation

Quantum chemical study was carried out using density function theory (DFT) method, with hybrid function of Becke three parameters Lee, Yang and Parr (B3LYP) with basis set 6-31G (d).[13] All the calculations were calculated with the help of Gaussian 03 software package. The quantum chemical parameters obtained were E_{HOMO}, E_{LUMO}, E_{LUMO}–E_{HOMO} (ΔE).

$$\Delta E = E_{LUMO} - E_{HOMO} \quad (4)$$

2.1.6. Molecular dynamic simulations

Forcite module in the Material Studio Software 7.0 from BIOVIA-Accelrys, USA was adopted in performing the Molecular dynamics (MD) simulations[14]. The simulation was carried out with Fe (110) crystal with a slab of 5 Å. The Fe (110) plane was enlarged to a (10 × 10) supercell to provide a large surface for the interaction of the MEP.The interaction energy ($E_{interaction}$) of molecules with Fe surface was obtained using the following equation:

$$E_{interaction} = E_{total} - (E_{Fe\ surface} + E_{molecule}) \quad (12)$$

where E_{total} is the total energy of the molecules and the metal surface system; $E_{surface}$ is defined as the energy of metal surface without adsorption of molecules and $E_{molecule}$ is the energy of isolated molecules.

The binding energy is the negative of the interaction energy and is given as:

$E_{binding} = -E_{int}$

3. RESULT AND DISCUSSION

3.1.Gravimetric measurement

3.1.1. Effect of inhibitor concentration

The variation of inhibition efficiency with inhibitor concentrations is shown in Fig. 2a. It is observed from figure that the inhibition efficiency increases as the concentration of inhibitor increases. The maximum inhibition efficiency obtained for inhibitors (MEP) is 98.7% at different concentration range (25-100 mgL^{-1}).

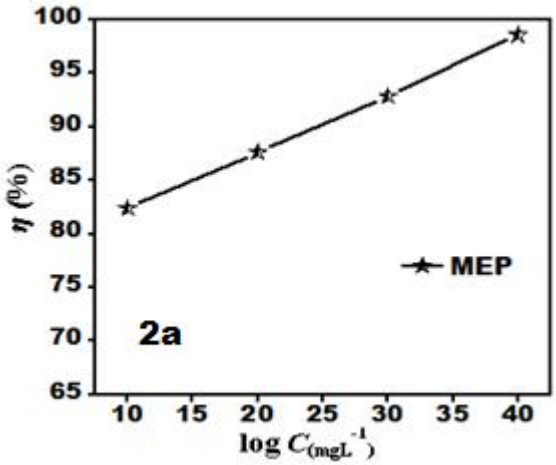

3.1.2. Effect of temperature

The variation in inhibition efficiency with temperature is shown in Fig. 2b. As observed from the figure the inhibition efficiency decreases from 98 to 65 % in the temperature range of 308 to 338 K. The decrease in efficiency with rise in temperature can be attributed to partial desorption of MEP molecules from the metal surface [15]. The temperature dependency of (corrosion rates) C_R was estimated using Arrhenius equation.

$$\log C_R = \frac{-E_a}{2.303RT} + \lambda \qquad (14)$$

where, E_a is the activation energy of the corrosion process, R is the gas constant, and λ is the Arrhenius pre-exponential factor.

The activation energies (E_a) values were calculated by plotting a graph between log C_R and $1/T$ at an optimum concentration of inhibitors and are shown Fig 2c. A straight line was observed with a slope of $E_a/2.303R$. The calculated values of E_a for in the absence and presence of inhibitor molecules are shown in Table 2. From the result it is revealed that E_a values in presence of MEP is higher than in their absence, which is due to the formation of physical barrier for charge and mass transfer created by adsorbed inhibitor molecules [15].

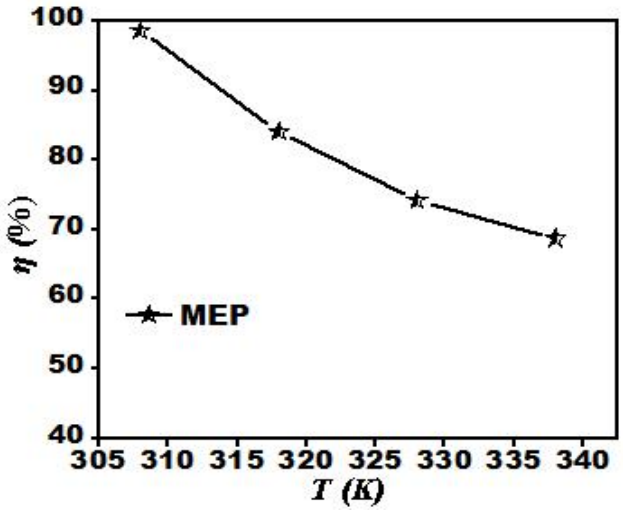

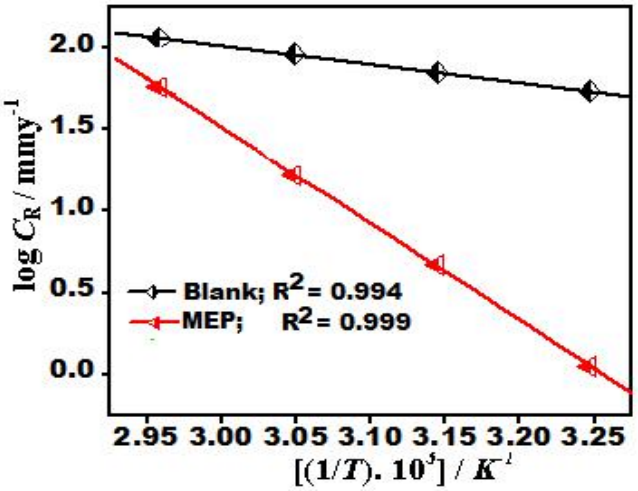

Table 2: Thermodynamic parameters for the adsorption of inhibitor on mild steel in 1M HCl at different concentration AT (100 mg L^{-1}) of MEP at 308K

Inhibitor	K_{ads} (10^4 M^-)	$-\Delta G^\circ_{ads}$ (kJ mol^{-1})	E_a (kJ mol^{-1})
Blank	----	----	28.74
MEP	2.5	39.26	120.04

3.1.3. Adsorption isotherm

Adsorption isotherm experiment was carried out to understand the mechanism of corrosion inhibition and interaction of inhibitor molecules with the metal surface. Various isotherms namely Langmuir, Temkin and Frumkin were fitted. The best fit was obtained for Langmuir isotherm. Langmuir adsorption isotherm is represented by the following equation [16]

$$\frac{C_{inh}}{\theta} = \frac{1}{K_{ads}} + C_{inh} \qquad (15)$$

Where K_{ads} is the adsorption equilibrium constant, C represents the concentration of the inhibitor and θ is surface coverage value. A straight line was observed by plotting a graph between log C_{inh}/θ vs. C_{inh} as shown in Fig 2d, which suggested the adsorption of inhibitor molecules on the metal surface obeys Langmuir adsorption isotherm.

The values of K_{ads} in association with the standard Gibbs free energy of adsorption ΔG^{o} (ads) was obtained from the Langmuir adsorption isotherm by the following equation:[16]

$$K_{ads} = \frac{1}{C_{(sol.)}} \exp\left(\frac{\Delta G^{0}_{ads}}{RT}\right) \quad (16)$$

Where R is universal gas constant, T is the absolute temperature and C is the concentration of water (1000 g/L). The values of K_{ads} is representing here in $g^{-1}L$, thus in this equation, the concentration of water is taken in g/L (1000 g/L) in the place of 55.5 mole/L. The values of K_{ads} and $\Delta G^{o}_{(ads)}$ are reported in Table 2. The calculated values of Kads and ΔG^{0}ads are given in Table 2. Generally, the higher value of Kads associated with strong adsorption and higher inhibition. which is accordance with the order of inhibition efficiency. In the present study, the value of ΔG^{0}ads is 39.26kJ mol^{-1}, signifying that inhibitor adsorb on mild steel surface in by mixed mode involving physiochemical mechanism [17]

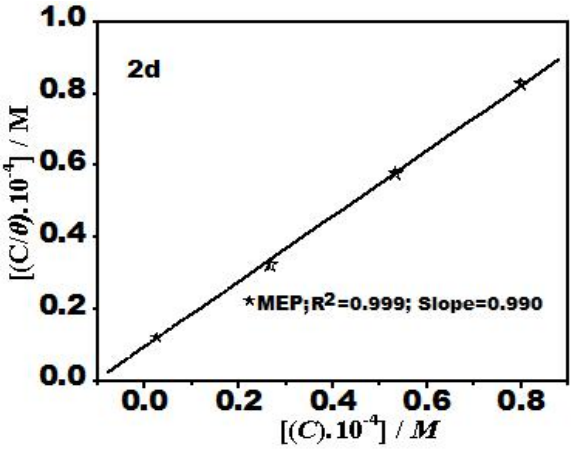

3.2. Electrochemical study

3.2.1. Electrochemical impedance spectroscopy

The corrosion behavior of mild steel in 1 M HCl in absence and presence of MEP was investigated by EIS after immersion for 30 min at 308 K. Nyquist plots of mild steel at different concentrations of inhibitors are given in Fig.3a. Inhibition efficiency can be calculated from Nyquist by using the following equation:

$$\eta\% = \left(1 - \frac{R_{ct}}{R_{ct(i)}}\right) \times 100 \quad (1)$$

where $R_{ct(i)}$ and R_{ct} are the charge transfer resistance in presence and absence of MEP, respectively. With the addition of the MEP the value of the impedance response of mild steel in acid solution was significantly changed as compared to the blank. The Nyquist plots were composed of one depressed capacitive loop at the higher frequency range (HF) and this may be attributed to the

charge transfer reaction. The appropriate circuit for studies is shown in Fig. 3b, it consists of constant phase element instead of capacitive element. The admittance, Y_{CPE}, and impedance, Z_{CPE}, are given and expressed as [18]:

$$Y_{\mathrm{CPE}} = Y_0 (j\omega)^n \tag{2}$$

And

$$Z_{\mathrm{CPE}} = \left(\frac{1}{Y_0}\right)\left[(j\omega)^n\right]^{-1} \tag{3}$$

where Y_0 is the amplitude comparable to a capacitance, j is the square root of -1, ω is angular frequency ($\omega = 2\pi f_{max}$) , n is the phase shift, which can be used as a gauge of the heterogeneity or roughness of the mild steel surface [36]. Depending on the value of n, CPE can represent resistance (n = 0, $Y_0 = R$), capacitance (n = 1, $Y_0 = C$), inductance (n = -1, $Y_0 = L$) or Warburg impedance (n = 0.5, $Y_0 = W$).

Inhibition efficiencies and other impedance parameters like R_s, R_{ct}, Y_0 and n, obtained from fitting the recorded EIS data using the equivalent circuit are listed in Table 3. The double layer capacitance (C_{dl}) values can be calculated from CPE parameter values Y and n using the given equation [16].

$$C_{dl} = \frac{Y\omega^{n-1}}{\sin\left(n(\pi/2)\right)} \tag{4}$$

As from the Table 3, it was found that the value of R_{ct} increased in the presence of MEP as compared to blank. In addition, the value of the proportional factor Y_0 of CPE varies in a regular manner with inhibitor concentration. The change of R_{ct} and Y_0 values can be related to the gradual replacement of water molecules by inhibitor molecules on the mild steel surface and consequently leads to decrease the number of active sites necessary for the corrosion reaction. The increase in R_{ct} value can be explained by the formation of protective film on the metal/solution interface. Moreover, the values of double-layer capacitance, C_{dl}, decreased in presence of inhibitors. The decrease in C_{dl} is probably due to a decrease in local dielectric constant and/or an increase in the thickness of a protective layer at electrode surface[19].

Bode plot in absence and presence of different concentration of MEP is given in Fig. 3c. In the higher frequency region the phase angle values go rapidly towards 0°. This is a response of resistive behavior and corresponds to the solution resistance. In intermediate frequencies region, the phase angle approaching -90°. This is a characteristic response of capacitive behavior at intermediate frequencies.

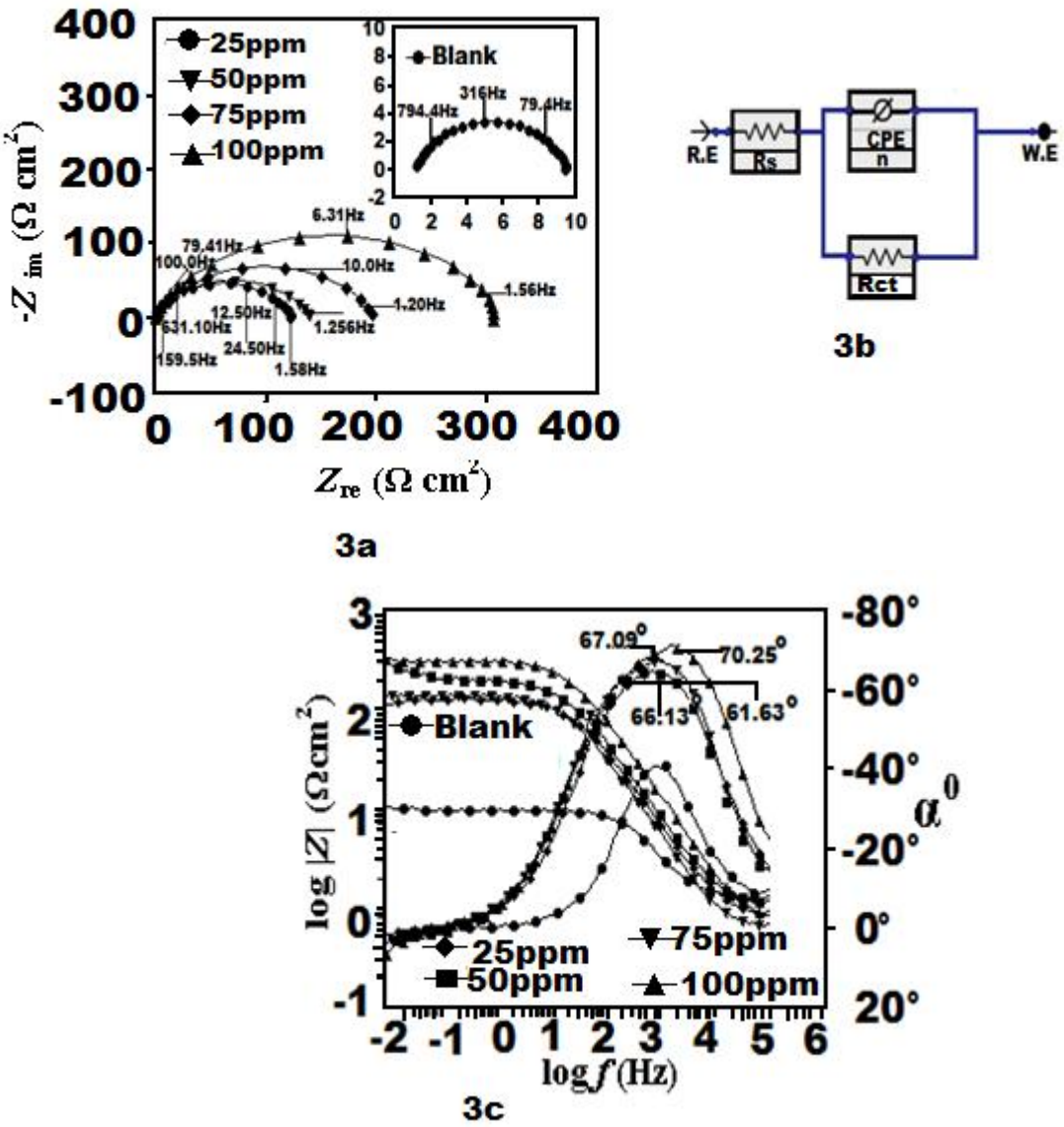

Fig 3

Table 3: Electrochemical impedance parameters (±SD) for mild steel in 1M HCl in absence and presence of different concentration (25-100 mg L^{-1}) of MEP at 308K

C_{inh} (mgL^{-1})	R_s (Ω)	R_{ct} (Ω cm^2)	*n*	C_{dl} (μF/cm^2)	*η* (%)
Blank	0.8(0.002)	9.0 (0.005)	0.798	137.9	----
25	1.01(0.002)	130.9(0.003)	0.824	48.3	93.1

50	0.5(0.002)	150.5(0.005)	0.847	46.1	94.0
75	0.9 (0.002)	209.1(0.003)	0.872	40.5	95.6
100	1.4 (0.002)	310.5(0.005)	0.882	23.6	97.1

3.2.2. Potentiodynamic polarization study

Potentiodynamic polarization experiment was performed to know the kinetics of cathodic and anodic reactions. The polarization curves in the absence and presence of different concentration of MEP in 1 M HCl solution are shown in Fig. 4 and their corresponding data are listed in Table 4.
The values of η % were calculated and given by the following equation:

$$\eta\% = \left(1 - \frac{I_{\text{corr(i)}}}{I_{\text{corr}}}\right) \times 100 \quad (5)$$

where I_{corr} and $I_{corr(i)}$ are the uninhibited and inhibited corrosion current densities, respectively. From the Table 4 it has been observed that i_{corr} for mild steel in 1 M HCl solutions decreases with the addition of MEP. This decrease in i_{corr} in the presence of MEP occurs due to its adsorption on the mild steel surface. Also both the anodic and cathodic curve are shifted towards lower current density, suggesting that inhibitors are reducing both anodic and cathodic reactions[20].

The data in Table 4 for corrosion potential (E_{corr}) shows that there is a shift in the E_{corr} values towards cathodic region. So, it could be said that inhibitors are mixed type inhibitors but predominantly cathodic.

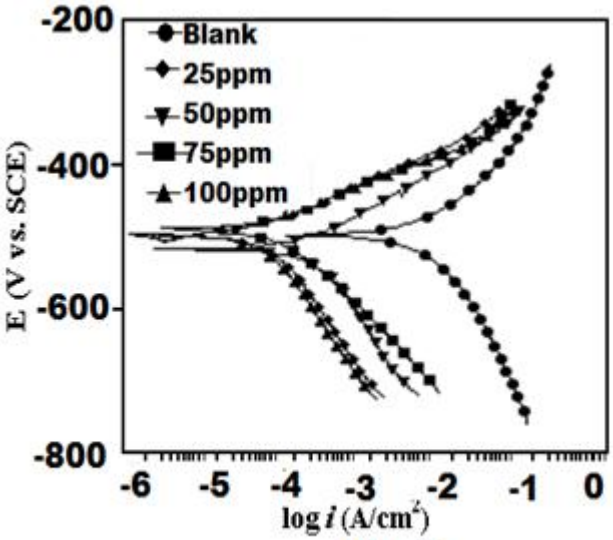

Fig- 4

Table 4: Potentiodynamic polarization parameters (±SD) for mild steel in 1M HCl in absence and presence of different concentration (25-100 mg L^{-1}) of MEP at 308K

Inhibitor	E_{corr} (mV/SCE)	i_{corr} (μA/cm^2)	β_a (mV/dec)	$-\beta_c$ (mV/dec)	η (%)
Blank	-445	1320(0.003)	85.7	100.8	----
25	-489	60.0(0.002)	81.6	142.1	93.2
50	-497	52.0(0.002)	83.3	158.8	94.1
75	-490	40.0(0.002)	82.5	141.3	95.5
100	-492	23.0(0.003)	87.5	152.5	97.4

3.3. Surface measurement

3.3.1. SEM and AFM analysis

The SEM images of inhibited and uninhibited mild steel specimens after 3h immersion time are shown in Fig.5 (a-b). it can be seen from the Fig 5a the mild steel specimen of uninhibited sample is highly damaged due to free acid corrosion. Moreover, the SEM image of the metallic specimen in presence of MEP is smoother than the absence of MEP inhibitor..

The AFM micrographs of mild steel specimens in the absence and presence of optimum concentrations of MEP are shown in Fig. 6(a-b). The micrograph of the mild steel surface in absence of MEP is 400 um and in presence of MEP is 30um. The results of SEM and AFM further corroborate the formation of protective film on metal surface.

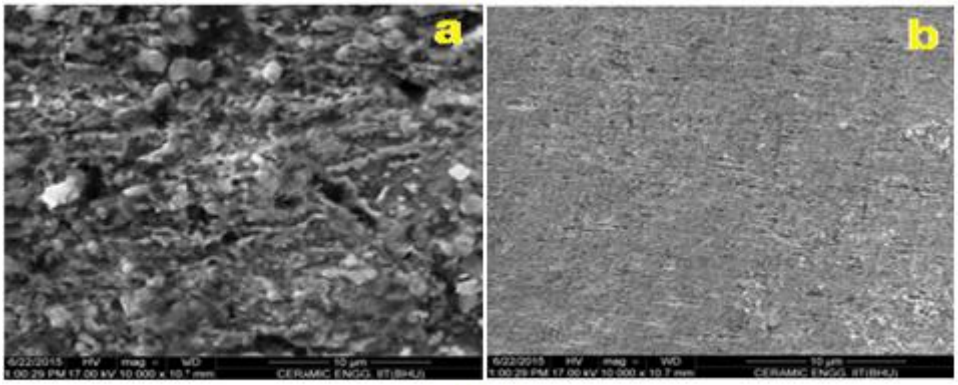

Fig 5

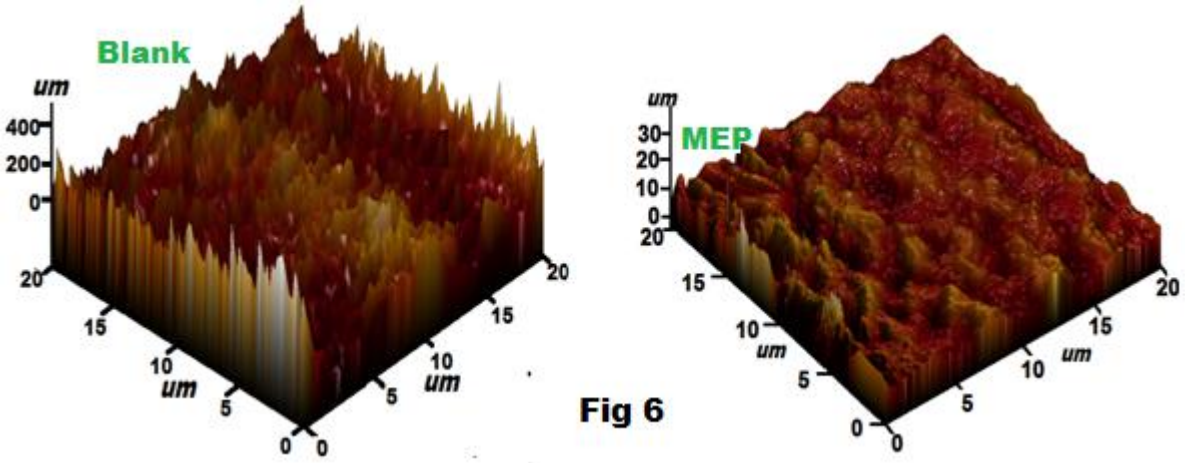

Fig 6

3.4. Quantum chemical calculations (Quantum chemical calculations of neutral inhibitor molecules)

For understanding the donor-acceptor relationship between the frontier molecular orbital's (FMOs) of the inhibitor molecules and the metallic surface, the study of the HOMO (the highest occupied molecular orbital) and LUMO (the highest unoccupied molecular) is very important. The Fig 2(a-c) shows the optimized structure, HOMO and LUMO of the MEP. Generally HOMO and LUMO represents the electrons donation and electron acceptor capacity of the molecules [20]. Higher E_{HOMO} value higher the electron donating ability of an inhibitor to the molecule. While the lower E_{LUMO} value greater chance to accept the electrons from metal surface during the back donation [15].]. It can be observed that in case of neutral MEP molecules, the HOMO electrons are distributed over the phenyl ring, nitrogen and oxygen atoms of the pyranopyrazole derivatives. And the LUMO, the electron distribution is confined on entire molecule except methoxy group attached to phenyl ring.

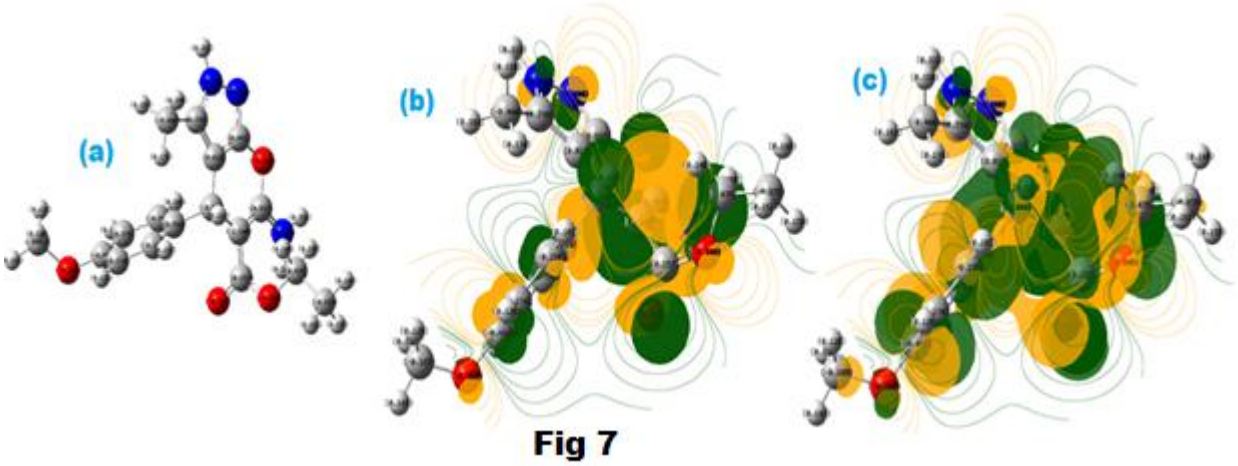

Fig 7

Table 5: Calculated quantum chemical parameters of neutral MEP DFT (6-31G, d, p)

Inhibitors	μ (Debye)	E_{HOMO} (eV)	E_{LUMO} (eV)	ΔE (eV)
MEP(neutral)	8.801	-6.485	-3.944	2.535

3.5. Molecular dynamics simulations

The interaction between the inhibitor molecule and metal was studied by molecular dynamics simulations [21]. Fig.8 represents the adsorption behavior of MEP molecules over the metal surface. It is clear that the studied inhibitor molecules are lying almost parallel to the metal. The calculated values of interaction energy ($E_{interaction}$) and binding energy ($E_{binding}$) are given in Table 6. The values of $E_{interaction}$ isnegative which suggest that adsorption is spontaneous [22]. The results are well correlated with experimental results.

Table 6: Interaction energies between the MEP and Fe (110) surface (kJ/mol) in gas phase

MEP	$E_{binding}$ (kcal/mol)	E_{inter} *(kcal/mol)action*
MEP(neutral)	183.53	-183.56

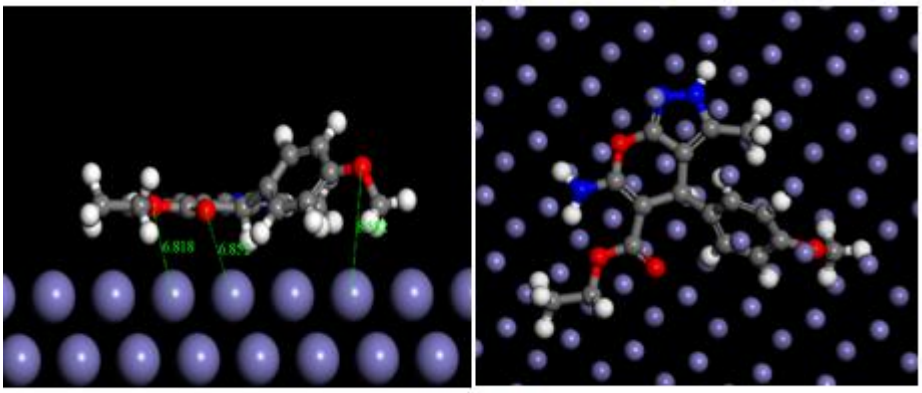

Fig 8

4. CONCLUSIONS

- Electrochemical impedance spectroscopic study revealed that MEP inhibits metallic corrosion by adsorbing at metal/ electrolyte interfaces and thereby enhancing the surface resistance.

- Potentiodynamic polarization study showed that MEP acted as mixed type inhibitors but predominantly behaved as cathodic inhibitors.

- AFM and SEM studies confirmed formation of adsorbed film on the metal surface and followed Langmuir adsorption isotherm.

- In all the tested methods, increase in the MEPs concentration leads to increase the inhibition efficiency and decrease in the corrosion rates at the different concentration range (25-100mgL^{-1}).

- Experimental results were supported by DFT based quantum chemical calculations and molecular dynamics simulations. Both experimental and theoretical results showed good agreement.

.

ACKNOWLEDGMENTS

The author Parul Dohare gratefully acknowledges the financial support of the ministry of Human Resources and Development (M.H.R.D.), New Delhi for providing the Senior Research Fellowship.

REFERENCES

[1] M.G. Hosseini, M. Ehteshamzadeh, T. Shahrabi, Electrochim. Acta 52 (2007) 3680-3685.

[2] H.B. Fan, C.Y. Fu, H.L. Wang, X.P. Guo, J.S. Zheng, Br Corros J. 2002; 37:122–125

[3] M. Behpour, S.M. Ghoreishi, A. Gandomi-Niasar, N. Soltani, M. Salavati-Niasari, Journal of Materials ScienceJ. Mater. Sci. 44 (2009) 2444.

[4] N. M. El-Haddad, A.S. Fouda, J. Mol. Liq, 209 (2015) 480–486

[5] M. Ozcan. J Solid State Electrochem 12, 1653,(2008)

[6]. G. Avcı, Colloids Surf. A Physicochem. Eng. Aspects 317 (2008) 730–736.

[7]. A. Döner, R. Solmaz, M. Özcan, G. Kardas , Corros. Sci. 53 (2011) 2902–2903.

[8] S. Gogoi, C. G. Zhao, Tetrahedron Lett. 2009 May 13; 50(19): 2252–2255.

[9] D. K. Yadav and M. A. Quraishi, | Ind. Eng. Chem. Res. 2012, 51, 8194−8210.

[10] I.B. Obot, Z.M Gasem. Corros. Sci. 83 (2014) 359-366.

[11] A. El-Assaly.Samy, Der Pharma Chemica, 2011, 3 (5):81-86

[12] ASTM, G 31–72, American Society for Testing and Materials, Philadelphia, PA, 1990.

[13] A.D.Becke, 1993, J. Chem. Phys. 98, 5648

[14] J. P. Zeng, J.Y. Zhang, X.D. Gong, Compt. Theo. Chem. 963, (2011) 110-114.

[15] P. Dohare, K. R. Ansari, M.A. Quraishi, I.B Obot, J. Ind. Eng. Chem. 52 (2017) 197–210

[16] N.Chaubey, DK. Yadav, VK.Singh, MA. Quraishi, http://dx.doi.org/10.1016/j.asej.2015.08.020

[17] P. M Wadhwani, D. G Ladha, V. K, Panchal, N.Shah, K,2015, RSC Adv. 5, 7098

[18] D.K Yadav, D.S Chauhan, I Ahamad, M.A Quraishi, RSC Adv. 3 (2013)632– 646

[19] M. Moradi, J. Duan, X. Du, Corros. Sci. 69 (2013) 338–345.

[20] B. Gomez, N. V. Likhanova, M. A. Dominguez-Aguilar, R. V. A. Martinez-Palou, J. Gasquez, J. Phys. Chem., 110 (2006) 8928–8934

[21] J.J. Fu, H. Zang, Y. Wang, S. Li, T. Chen, X. Liu, Ind. Eng. Chem. Res. 51 (2012) 6377–6386.

[22] Y .Sasikumar, A.S Adekunle, L.O Olasunkanmi, I.Bahadur,. R Baskar, M Kabanda. I.B Obot, E.E EbensoJ. Mol. Liq 211 (2015) 105–118.